APPLICATION OF AASHTO FATIGUE DESIGN PROVISIONS FOR STEEL ORTHOTROPIC BRIDGE DECKS

Introduction

Prefabricated modular steel orthotropic deck panels can provide an effective solution for accelerated construction of highway bridges. This deck form has been widely used as new design and rehabilitation of long span signature bridges and movable bridges, as temporary structures in battle zones and large urban construction projects, and as emergency bridge replacements in the aftermath of natural disasters. The light weight redundant deck form helps in increasing the longevity of a bridge by reducing dead load stresses on the main supporting elements and by employing a thin overlay that promotes durability, improved riding quality and low maintenance. In-service performance and limited laboratory tests have demonstrated that if adequately designed and properly fabricated, the orthotropic deck is the only system likely to facilitate accelerated bridge construction and provide a service life exceeding 100 years [1], as is increasingly being advocated by the Federal Highway Administration and other transportation agencies around the country to minimize life cycle costs of the nation's growing bridge infrastructure. Despite the advantages and successful implementation of this deck system around the world, use of orthotropic deck form in the United States has been limited, primarily due to relatively high initial cost owing to intensive fabrication, and more importantly due to concerns regarding higher possibility of in-service fatigue cracking from a large number of welded connections if not adequately designed and/or fabricated. The most severe of these welded details are the bulkhead/sub-floor beam-to-rib connections and the rib-to-deck welds that are subjected to in-plane and out-of-plane deformations localized under wheel loads [2].

Per AASHTO LRFD Bridge Design Specifications [3], fatigue design of steel bridges is performed using nominal stress versus life (S-N) curves that were mostly developed based on fatigue test results of beam specimens having different detail categories of differing notch severity. Nominal stresses are typically determined using simple strength of material calculations based on applied loading and nominal section properties, but considering the gross geometric changes at a section, which locally magnify or decrease the nominal stress. Because of the complex geometries and distribution of stresses in orthotropic decks, however, nominal stresses in orthotropic deck elements cannot be easily defined or computed. As such, the traditional nominal stress based fatigue design provisions of the AASHTO Specifications are not readily applicable to the orthotropic deck details, and therefore designing orthotropic decks requires advanced analysis and often full scale proof testing in the laboratory. The lack of universally accepted standard guidelines for fatigue design based on advanced analyses and the associated increased efforts for such analyses also increased the impediments to the wider acceptance and implementation of orthotropic bridge decks in the United States.

Recently, local stress based fatigue design guidelines for orthotropic decks were incorporated into the AASHTO Specifications [3-5]. These guidelines were incorporated from the International Institute of Welding recommendations [6], without any experimental or analytical verification of these guidelines for large scale application, particularly on orthotropic decks. According to the AAHTO recommendations, the local stress (referred in the specification as the local structural stress) for fatigue design is to be determined based on advanced analyses using finite element methods (FEM), where the FE model is developed using solid or shell elements of acceptable formulation to capture steep stress gradient. The FE model is recommended to have a mesh density of t × t, where t is the thickness of the plate element. The local structural stress is to be estimated perpendicular to the weld toe and determined by extrapolating stresses obtained from the finite element analysis (FEA) results at the reference points located on the surface of the element at a distance of 0.5 t and 1.5 t measured perpendicular from the weld toe. Thus, the local structural stress, σ, at the weld toe is determined as:

$$\sigma = 1.5 \cdot \sigma_{0.5} - 0.5 \cdot \sigma_{1.5} \qquad (1)$$

where, $\sigma_{0.5}$ is the surface stress at a distance of 0.5 t from the weld toe and $\sigma_{1.5}$ is the surface stress at a distance 1.5 t from the weld toe. In the specification commentary, it has been suggested to use this local stress in conjunction with the AASHTO Category C design curve, without any distinction for finite and infinite life assessments. It should be noted that this local stress-based approach, borrowed from application in other industries, had been proposed by calibrating against toe cracking in small scale specimens. A local stress-based approach, using the stress at a

reference point on the surface ahead of the weld toe, was originally developed and successfully applied for fatigue cracking at the weld toe of tubular structures in the offshore industry [7], where significant out-of-bending arises at the connections to maintain compatibility of deformation between the components. Research efforts of developing local stress based approaches for plated structures have produced mixed results, particularly where the out-of-plane bending effects are nominal and in-plane stress components are dominant [7]. Application of this methodology for fatigue cracking from weld root and specifically for infinite life design (i.e., no fatigue crack growth at all) is questionable.

An alternative local stress based approach was successfully used by Roy and Fisher [8] and Roy et al. [9] for assessing infinite life fatigue resistance of welded connections. This approach considers the fatigue effective local stress at the weld toe notch and compares it against the endurance limit of the material to suppress the possibility of cyclic crack initiation or propagation. A notch of 0.04 in (1 mm) radius is introduced at the toe of the nominal weld geometry, and the converged maximum (tensile) surface stress at the center of the rounded notch is used as the local stress (also defined as the notch stress) for assessment of infinite life fatigue resistance.

In this paper, the applicability of the newly introduced AASHTO fatigue design provisions are verified with respect to fatigue test results of two distinctly different welded steel orthotropic deck forms. These decks were evaluated by full scale laboratory testing at Lehigh University for two different performance objectives. One of the deck forms, identified as Deck A in the following, was tested for infinite life. The other deck form, subsequently identified as Deck B, was tested for finite life. The critical stresses in the decks were estimated by detailed three dimensional (3D) FEA and their fatigue performance was assessed based on the AASHTO provisions. In addition, the infinite life performance of Deck A was evaluated using the notch stress-based approach.

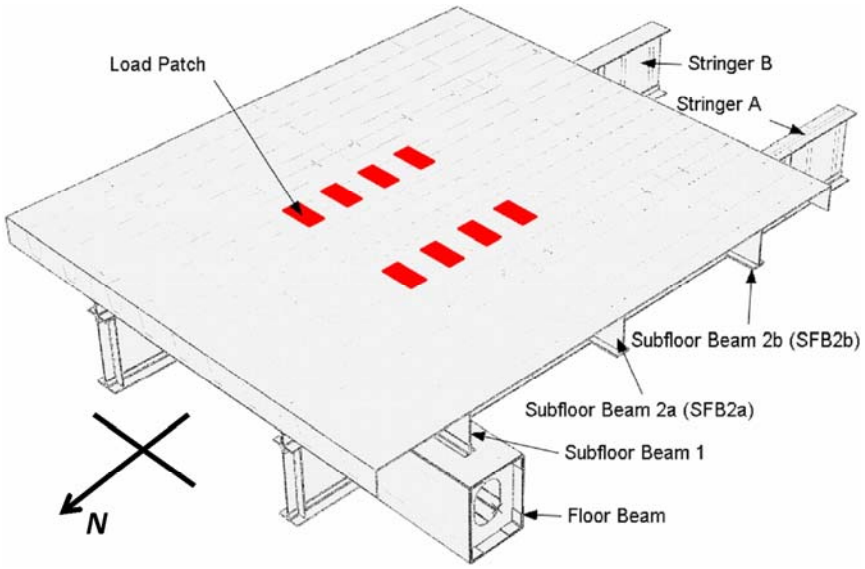

Figure 1 Global model of Deck A

Description of Prototype Deck Specimens

Deck A

Deck A was a full scale prototype of the replacement orthotropic deck for a signature bridge [10] that was designed integral with the floor framing system (Figure 1) and as such, exhibited a two-way behavior. Longitudinal plates called stringer extensions were welded to the deck plate and discretely fastened to the stringers along their centerline. The transverse subfloor beams spanned between these stringer extensions except at the floor beam locations, where they were supported by the floor beams. This deck specimen consisted of nine closed trapezoidal ribs passing uninterrupted through matching cutouts in three subfloor beams. Additional cutouts were provided in subfloor beams under the rib soffit. The subfloor beam-to-rib welded connection comprised a 4 in long complete joint penetration (CJP) groove-weld at the cutout, transitioning into a partial joint penetration (PJP) weld above. Full depth bulkhead plates were provided in the ribs at the intersection with the subfloor beams. The plate thicknesses

were: $^{5}/_{8}$ in for the deck plate; $^{5}/_{16}$ in for ribs; $^{5}/_{8}$ in for bulkhead plates; and $^{7}/_{8}$ in for the subfloor beam web. The overall dimension of the deck was 25 ft 7 in long × 22 ft $3^{1}/_{8}$ in wide.

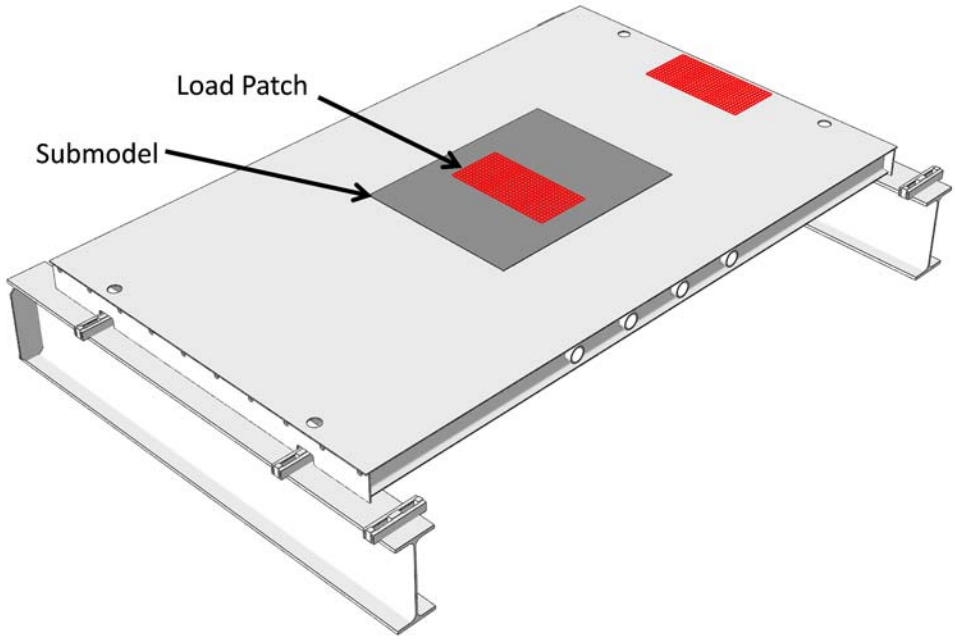

Figure 2 Global model and submodel of Deck B

Deck B

Deck B was a standard open rib orthotropic deck typically used in one-way simply supported configuration for temporary construction (Figure 2). This deck consisted of 10 rolled I-shaped ribs (also called stringers) and $^{3}/_{16}$ in thick deck plate. In the transverse direction, the stringers were interconnected by four hollow circular tubes passing centrally through their webs and welded to the stringer webs. These tubes were provided symmetrically near the mid span. End plates were provided at each end of the stringers.

Finite Element Analyses

Three dimensional FEA of the decks were conducted using a commercially available package ABAQUS [11]. The analyses were performed in multi levels. In the first level, a global model of the deck along with the supporting floor framing was analyzed, replicating the test setup. In the subsequent levels, progressively smaller local models (submodel) of the critically stressed areas of the deck were analyzed for further refined assessment of local stresses at the welded connections. All models were developed using 20 node second order solid serendipity elements incorporating isoparametric reduced integration formulation.

The global model included all features of each component. The welded and/or bolted connections were not modeled; instead all welded and/or bolted connections in a component were considered as integral and all bolted connections between components were displacement constrained. The submodel analyses employed solid-to-solid submodeling, where the submodels were driven by the displacement solutions of the global model or the previous level submodel at the interfaces. The welds were included only in the submodels as per the nominal size indicated in the fabrication drawings. The weld toe for all submodels was modeled as a sharp corner (zero notch radius), except for those analyzed to determine the notch stress (for assessing infinite life fatigue performance), where a 0.04 in (1mm) rounding was introduced. The welds were modeled with full penetration at the weld root.

All analyses were linear elastic. Widely accepted linear elastic material properties of steel were used for the analyses. The modulus of elasticity and Poisson's ratio of steel were assumed as 29000 ksi and 0.3, respectively. The loads were applied as pressure on 10 in × 20 in patches, simulating tire contact areas as per the AASHTO

specifications [3]. The disposition of loads and the boundary conditions are discussed further in the following for individual decks.

All analyses were conducted on a distributed memory parallel execution computer cluster of 16 machines, each having eight central processing units (cpu).

FEA of Deck A

The global model of Deck A is shown in Figure 1.The model included the deck specimen, and the floor beam and the stringers that were considered as part of the test setup. The nominal mesh size was 1 in and the model consisted of 768,576 elements, 4,970,631 nodes, and 14,911,899 degrees of freedom.

The boundary conditions were defined consistent with the test setup [10]. The west end of the floor beam was assumed fixed to simulate the rigid connection of the floor beam to the laboratory wall. The east end of the floor beam and the south end of the stringers were assigned displacement boundary conditions. In the laboratory tests, the under deck actuators were used to displace the stringers and the floor beam vertically.

The deck was analyzed for the same loading as the laboratory tests [10], where a pair of adjacent actuators was loaded simultaneously in sequence to simulate the passage of a tandem axle. The load from each actuator was transferred to the deck using spreader beams and loading blocks at each end of the spreader beams, which simulated truck axles and wheels respectively. To assess infinite life fatigue performance, this deck was tested to a load level equivalent to 2.25 times AASHTO fatigue design truck corresponding to Fatigue I limit state for orthotropic decks, and an additional 15% impact [10]. The rear axle load of the AASHTO fatigue truck was split into a tandem configuration as per the latest AASHTO provisions [3-5]. Accordingly, the global model was analyzed for a pressure of 105 psi applied on each of the four load patches in each load step as shown in Figure 1.

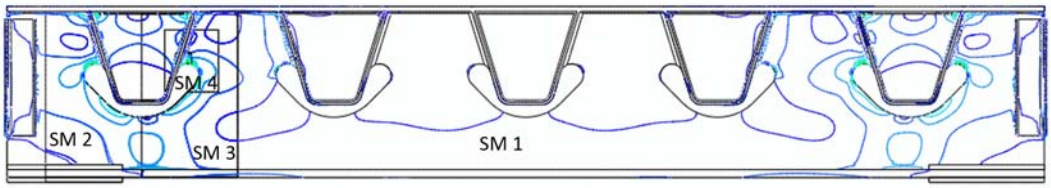

Figure 3 Superimposed principal stress contours for submodels of Deck A at intermediate subfloor beam

The FEA results of the global model identified high stress concentrations in the intermediate subfloor beam at the cutout locations, in the vicinity of the rib-to-subfloor beam welded connection. Thus, the submodel analyses focused on this location. Originally, five levels of submodels were analyzed where the mesh sizes were progressively reduced by half to obtain a converged solution in the vicinity of the critical welded details for assessment of infinite life fatigue performance. These submodels are identified in Figures 3 and 4. Subsequent to the incorporation of the orthotropic deck design provisions in the AASHTO specifications, the second level submodel was again analyzed with a mesh size meeting the requirements of the AASHTO specifications.

The first level submodel (SM1) included a 135 in length of the deck symmetric about the critically stressed intermediate subfloor beam between the stringer extensions containing five ribs. The second level submodel (SM2) considered only a 25 in length of the critically stressed ribs, the deck, and part of the subfloor beam with half the rib spacing on either side of the rib centerline. The third level submodel (SM3) considered only the west half of rib 7, in which the cutout was subjected to tensile stresses. This model considered a 12.5 in length of the deck. The fourth level submodel (SM4) was only 9 in long and included a smaller region of the highly stressed region of the cutout. The fifth level submodel (SM5) included a 2.5 in × 2.0 in × 1.5 in segment at the cutout stress concentration. The nominal mesh size for SM1 was 0.5 in and for SM5 was 0.03 in. Submodels SM4 and SM5 were developed for assessment of infinite life fatigue performance of the rib-to-subfloor beam welded connection according to the notch stress approach. A 0.04 in (1 mm) rounding was provided at the subfloor beam-to-rib weld toe in these submodels. As indicated earlier, SM2 was also reanalyzed for a nominal mesh size of $^{7}/_{8}$ in, consistent with the thickness of the subfloor beam web, as required by the AASHTO recommendations. This analysis was identified as SM2A.

FEA of Deck B

The global model of Deck B is shown in Figure 2. The model was as a true replicate of the test configuration including the deck and the supporting floor beams at each end. The average nominal mesh size was about 3 t × 3 t, where t was the thickness of each component. Only one element was provided through the plate thickness and the aspect ratio of the elements was limited to 4. The maximum and minimum corner angles of the elements were 110^0 and 65^0 respectively. The model consisted of 172,249 elements, 793,019 nodes, and 2,155,953 degrees of freedom.

Displacement boundary conditions restraining displacements in all three coordinate directions were imposed at the underside of the bottom flange of the floor beams to simulate seating on rigid pedestals in the test setup.

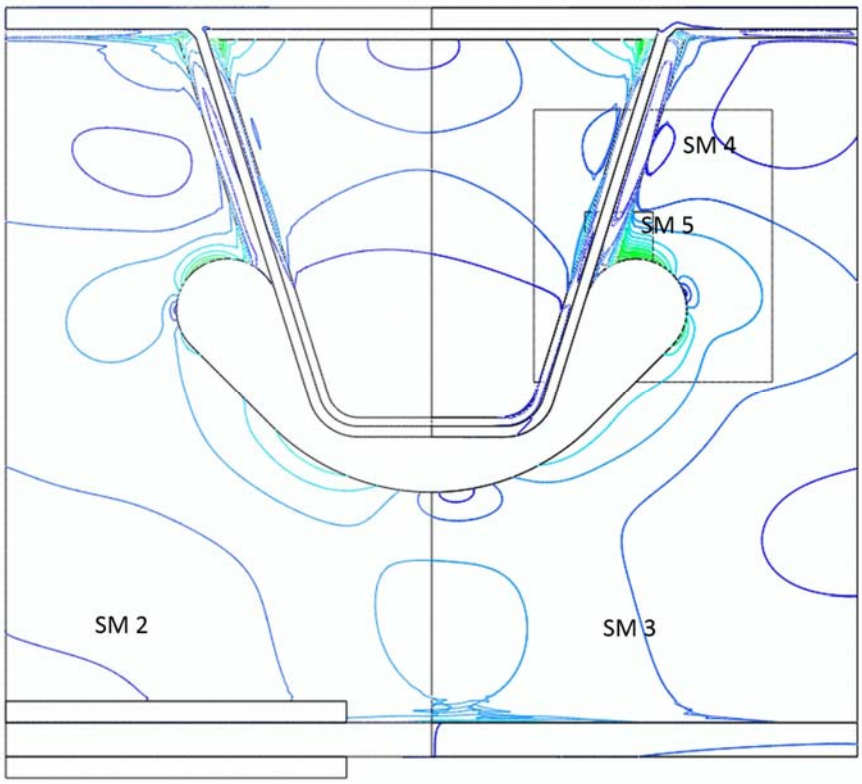

Figure 4 Superimposed principal stress contours for submodels of Deck A around cutout

The deck was analyzed for the same loading configuration as the test setup, where a pair of load patches simulating the tire contact of one side wheels of an AASHTO tandem axle was positioned most critically as shown in Figure 2. This deck was tested to determine its finite life performance and multiple specimens were tested at two load levels. One load level was equivalent to an AASHTO fatigue design truck scaled by the load factor of 0.75 for Fatigue II limit state, and included an additional 15% impact. The other load level was thrice this load and corresponded to a load equivalent to Fatigue I limit state for orthotropic decks. The rear axle load of the fatigue design truck was split into a tandem configuration as per the latest AASHTO provisions. The global model was analyzed for the higher load level, with applied pressure of 105 psi at each load patch.

The FEA result of the global model identified that the tube-to-stringer connections were the most critical details in the deck, due to out-of-plane distortion of the stringer web. A submodel was developed focusing on the critical tube-to-stringer connection for further refined assessment of local stress at this welded detail according to the AASHTO guidelines. The submodel contained a 30 in wide × 39 in long center part of the deck including three tubes, four stringers, and the deck plate, symmetric about the central loading patch (Figure 2). The average nominal mesh size for the submodel was about t × t, where t was the thickness of each component. Two elements were provided through the plate thickness and the aspect ratio of the elements was limited to 4. The maximum and minimum corner

angles of the elements were 99^0 and 65^0 respectively. The model consisted of 197,598 elements, 783,958 nodes, and 2,096,442 degrees of freedom.

Results and Discussions

Deck A

Superimposed principal stress contours obtained from the submodel analyses are shown in Figure 3 and 4. The plots of normal stress (S_{11}) profile along a path normal to the toe of the rib-to-subfloor beam weld, obtained from the submodel analysis results are shown in Figure 5. These plots demonstrate that S_{11} converged in SM3 for a mesh size of 0.25 in, which was $^2/_7$ of the plate thickness. The plots also showed that the stresses did not converge for a mesh size of t × t (0.875 in × 0.875 in) in SM2A, and a jagged stress variation was noted due to the relatively large mesh size. The origin of the path along the weld toe was determined from the FEA results of SM3, where the variation of S_{11} along the weld toe showed that this stress peaked at a distance of about 0.4 in from the cutout.

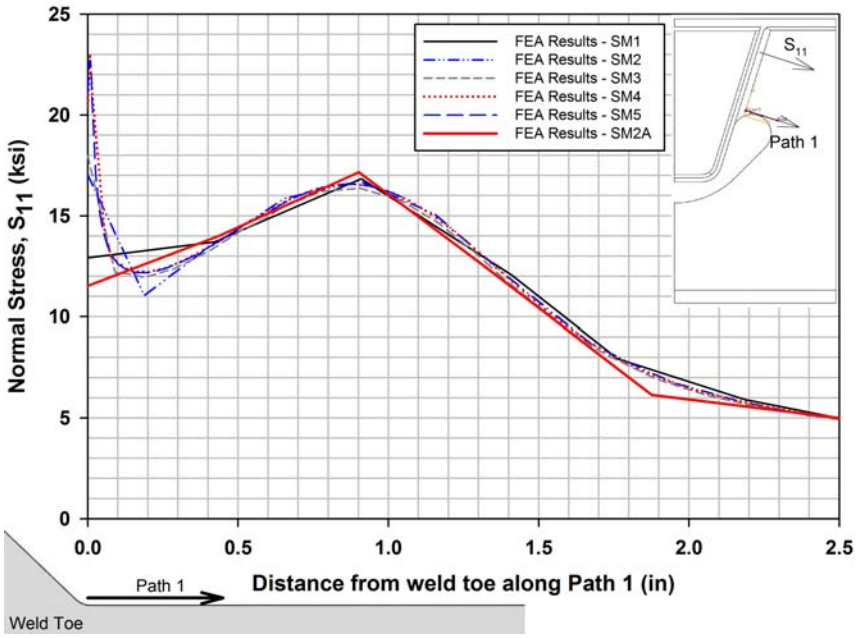

Figure 5 Variation of maximum S_{11} on the north face of subfloor beam in Deck A

As is seen from Figure 5 the normal stress S_{11} did not change monotonously. At the weld toe, a stress peak was noted due to the notch effect of the weld toe. It should be noted that this stress is theoretically infinite for a sharp notch of zero radius; a fictitious finite value is obtained corresponding to the FE mesh size and the approximation involved. Away from the weld toe, this stress decayed rapidly consistent with the decay of the theoretically infinite stress ahead of a sharp notch, but increased again to another peak due to the stress concentration at the cutout. This stress concentration occurred at a distance of about 0.9 in away from the weld toe.

Following the AASHTO recommendations, the local structural stress at the weld toe was estimated from the FEA results of SM2A by extrapolating the surface stresses at 0.5t and 1.5t distance on a path perpendicular to the weld toe (Figure 6). As is evident, the reference points were located on either side of the peak stress due to the cutout and therefore, the local structural stress at the weld toe was influenced by the stress concentration resulting from the cutout geometry. This local structural stress at the weld toe was estimated using the equation (1) as 14.7 ksi, also illustrated graphically in Figure 6. It can also be seen that the estimated stress at the weld toe based on the t × t mesh density in SM2A was 11.6 ksi.

The full scale prototype of Deck A was fatigue tested for 5 million cycles and no cracking was observed when the test was terminated. In Figure 7, the calculated local structural stress from equation (1) is used to evaluate the fatigue performance of the rib-to-subfloor beam welded detail according to the AASHTO provisions. Since the extrapolated local structural stress range was well above constant amplitude fatigue threshold (CAFT) of AASHTO Category C

details (10 ksi), the subfloor beam-to-rib welded connection could develop fatigue cracking at the weld toe at a (finite) design life between of about 1.4 cycles. In view of the inherent variability in the fatigue test results associated with micro and macro discontinuities at the weld toe, the AASHTO Category C design curve in the finite life region exhibits a lower bound or 95% confidence on the 95% probability of survival life for the detail category. Thus, it is expected that a significant number of connections belonging to this population will not develop fatigue cracking at this life. However, the rib-to-subfloor beam connection survived 5 million cycles without any evidence of fatigue cracking, which exceeded the upper bound or 95% confidence on the 95% probability of failure life (approximately 2.4 million cycles) for the Category C details. Apparently, this connection was subjected to a stress range that was below its CAFT and therefore demonstrated infinite life. Thus, the applicability of the latest AASHTO provisions for assessing infinite life performance is questioned for this case.

An interesting observation is that the stress of 11.5 ksi at the weld toe, which was obtained from the SM2A results (Figure 7), was closer to the CAFT of Category C details (10 ksi) and was less than the CAFT of Category C′ details (12 ksi). The converged stress at the valley of the stress profile (Figure 6), where the influence of the weld toe notch dissipated, was approximately 12 ksi, which is almost the same stress at the weld toe provided by the SM2A results (Figure 7). Apparently, the stress at the weld toe obtained from SM2A captured the local structural stress sans the stress raising effect of the weld toe notch. This stress at the weld toe could be used as a better estimate of local stress for assessing the infinite fatigue life than the extrapolation procedure.

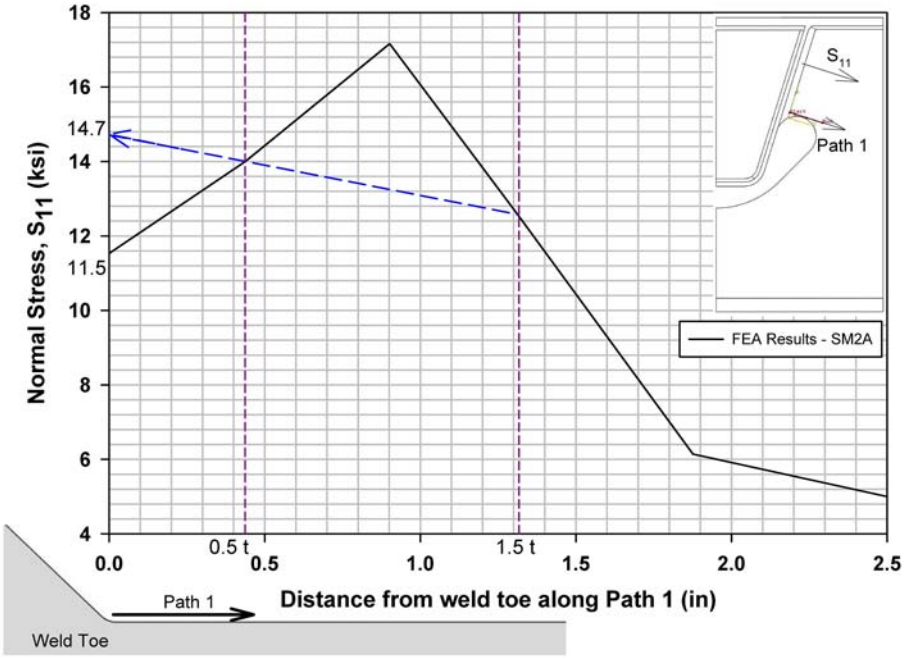

Figure 6 Local structural stress in Deck A as per AASHTO recommendations

The infinite life fatigue resistance of the rib-to-floor beam welded connection against fatigue crack growth from the weld toe was determined from the following equation [9]:

$$(\Delta F)_l = \frac{1}{3.2}\left[-\sigma_y + \sqrt{\sigma_y{}^2 + 4 \times S_e{}^2}\right] \qquad (2)$$

where, $(\Delta F)_l$ is the local infinite life fatigue resistance at the weld toe notch, σ_y is the yield strength of the material and S_e is the endurance limit of smooth specimens. The above relationship was simplified from a relationship developed by Roy and Fisher [8] as a function of the stress ratio (the ratio of stress range to minimum stress), the welding residual stress, the endurance limit, and the effective notch stress, for assessing CAFT of welded connections. In as-welded connections, tensile residual stresses are approximately equal to the yield stress of the material near the weld, which results in a local stress ratio in excess of 0.5. An endurance limit of 0.5 of the tensile

strength is generally assumed for structural steel. The fatigue effective notch stress then reduces to about 80% of the notch stress of the rounded weld toe.

The notch stress from the FEA results of SM5 was obtained as 21.5 ksi. For ASTM A709 Gr. 50 steel, assuming a nominal yield strength of 70 ksi and a nominal ultimate strength of 90 ksi, the local infinite life fatigue resistance at the weld toe notch was obtained as 27.9 ksi using equation (2). Indeed, the applied local notch stress range was less than the local fatigue resistance, indicating infinite life for the detail.

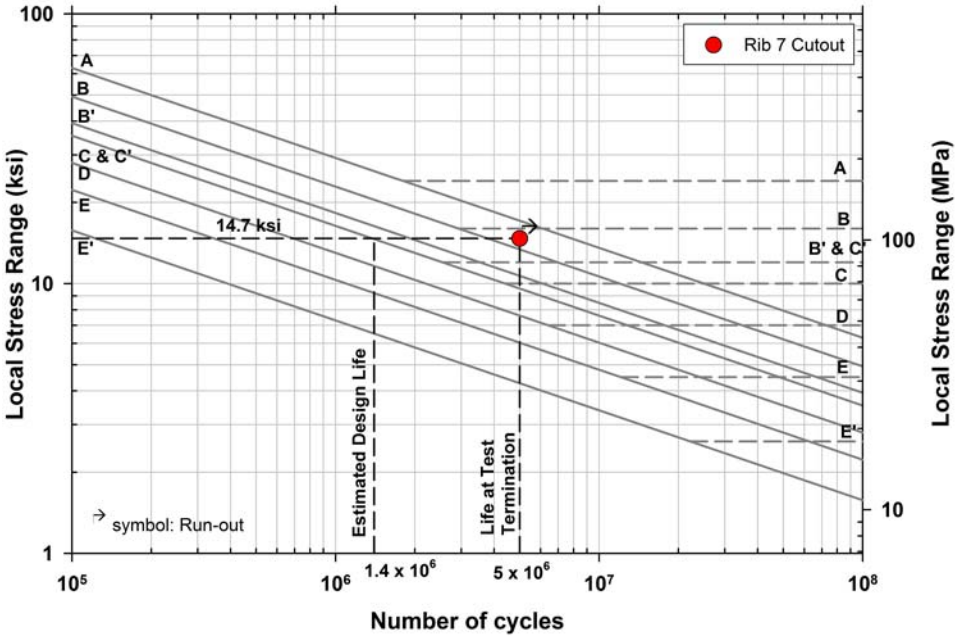

Figure 7 Evaluation of fatigue performance of Deck A as per AASHTO recommendations

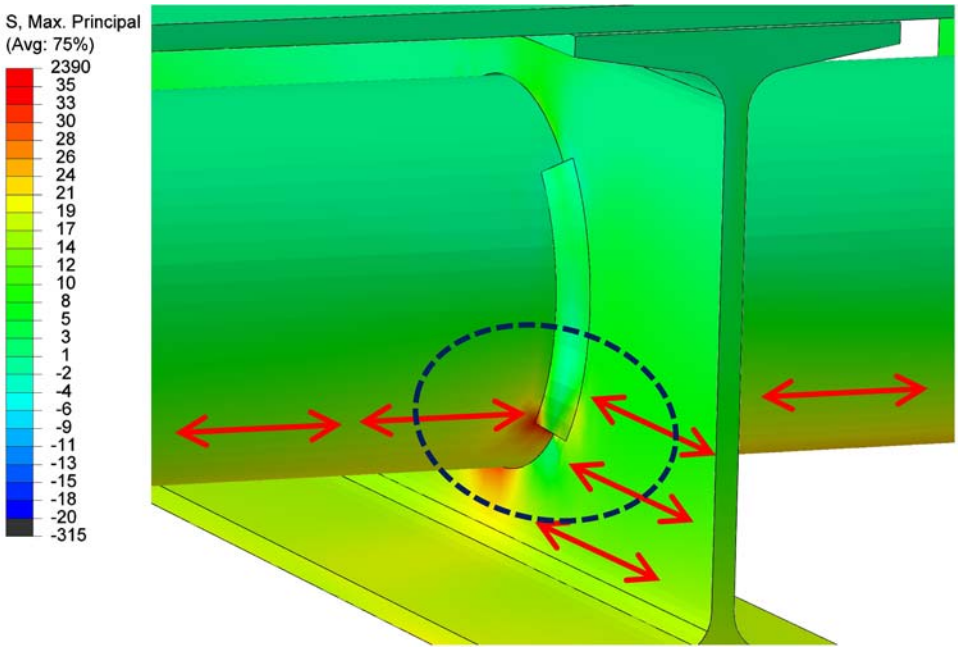

Figure 8 Contour of maximum principal stress at the stringer-to-tube weld in Deck B

Deck B

Figure 8 shows the contour of the maximum principal stress as determined from FEA results of Deck B at the critically stressed tube-to-stringer welded connection. Directions of principal stresses are also shown schematically on this figure. High stress concentration was noted at the stringer-to-tube weld toe on the tube near the lower termination, where fatigue cracks initiated in the specimens during laboratory testing. Significant local out-of-plane bending of the tube and the stringer was indicated by the FEA results, which caused the high stress concentrations at the weld termination.

Fatigue performance of the tube-to-stringer welded connection was evaluated based on the local structural stress determined at the weld toe on the tube, following the AASHTO recommendations. Since the maximum principal stress in the tube was almost normal to the weld toe on the tube, the local structural stress was extrapolated from the principal stresses at 0.5 t and 1.5 t ahead of the weld toe on the tube surface in a plane normal to the weld toe, where t was the thickness of the tube. Figure 9 shows the stress profile ahead of the weld toe and determination of the extrapolated local structural stress. Unlike Deck A, a monotonous stress gradient was seen at the weld toe region.

Fatigue test results of Deck B are plotted with respect to the local structural stress range in Figure 10 against the fatigue design curves of AASHTO specifications [3]. Two deck specimens were tested at the lower load level and one deck specimen was tested at the higher load level. As is evident, the fatigue life of the tube-to-stringer welded connection fell on the AASHTO Category C fatigue design curve in the finite life region. One specimen was identified a run-out when the fatigue test was terminated after 10 million cycles. The test results verified the applicability of AASHTO fatigue design provisions using local structural stress and the AASHTO Category C fatigue design curve for finite life. However, applicability of the guidelines for the infinite life region was questionable, since fatigue cracking was observed under a local structural stress range of 8.1 ksi, which was lower than the CAFT of AASHTO Category C, defined by the specification as 10 ksi.

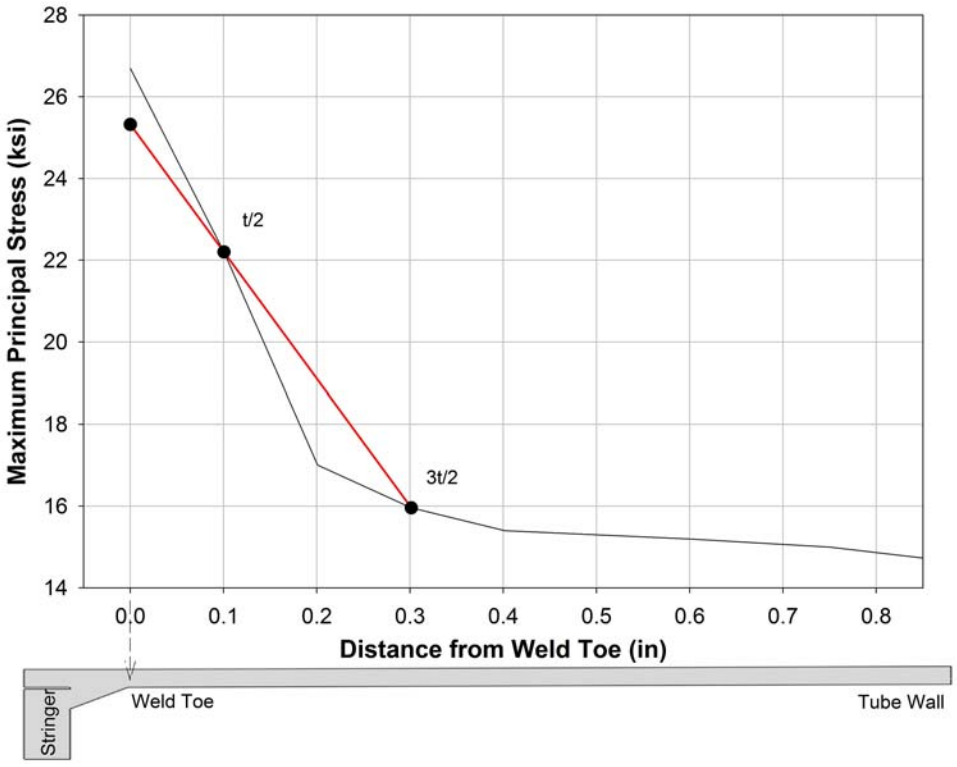

Figure 9 Local structural stress in Deck B as per AASHTO recommendation (for the larger applied load)

Conclusion

Applicability of the recently introduced local stress-based fatigue design provisions for orthotropic bridge decks in the AASHTO LRFD Bridge Design Specifications were investigated with respect to full-scale fatigue test results of two types of welded steel orthotropic decks that were designed and evaluated for finite and infinite life performances respectively. Three dimensional solid models of these decks in the test configuration and submodels of the critical details were analyzed by FEA, and their fatigue performance was assessed based on the local structural stress in conjunction with the Category C fatigue design curve, following the AASHTO specifications. These predictions were compared with the fatigue test results of the decks. The study verified that the finite life of the connection details against fatigue cracking from the weld toe could be predicted following the AASHTO recommendations, particularly when the local stress adjacent to the weld toe was significantly influenced by out-of-plane bending of the plate. The recommendations, however, were incapable of predicting the infinite life performance of the rib-to-subfloor beam and the tube-to-stringer connections investigated in this study. The exercise also showed that the stress at the weld toe obtained from the stress profile used for determining the local stress by extrapolation could provide a superior estimate of local stress for assessing the infinite fatigue life than the extrapolation procedure.

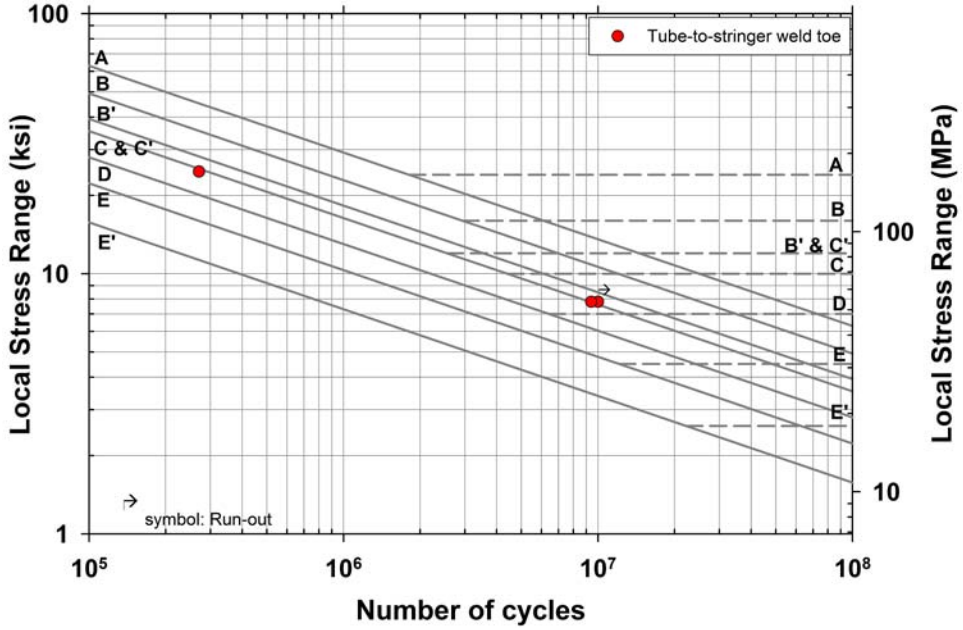

Figure 10 Evaluation of fatigue performance of Deck B as per AASHTO recommendations

Infinite life fatigue performance of a critical welded connection against fatigue cracking at the weld toe was evaluated by a local notch-stress based approach. This approach have been successfully used for assessing CAFT of welded cover plate and stiffener details in bridge girders and tube-to-transverse plate connections in highway sign, signal and high level luminaire support structures. As was demonstrated by this study, the local notch stress at the weld toe was able to correctly predict the infinite life performance of the rib-to-subfloor beam detail.

The primary reason for the inadequacy of the AASHTO recommendations in correctly assessing the infinite life performance of a welded connection is that the defined local structural stress had been postulated based on calibration with respect to the fatigue life associated with crack growth from the weld toe of a connection. This stress, computed based on extrapolation of stresses away from the weld toe, can capture the effect of significant out-of-plane bending stresses arising from the need to maintain compatibility of deformation between the connected components, or the connection geometry. To achieve infinite life, however, fatigue crack initiation and at the least the crack propagation at the weld toe should be suppressed. To this end, the local stress at the weld toe notch including the effect of the weld geometry is important.

It should be noted that the response of orthotropic deck details is characterized by local distortion under wheel loads [12-14], and therefore these details are subjected to number of fatigue effective stress cycles that are number of axle-

multiples of the truck traffic count. Accordingly, majority of the orthotropic bridge decks on the national highway network are expected to experience enough number of stress cycles requiring infinite life design against fatigue limit state. The AASHTO local stress-based fatigue design provisions for orthotropic decks should be supplemented with appropriate robust protocols for accurate and reliable infinite life design.

References

[1] Fisher, J.W., and Roy, S. (2010). "Fatigue of steel bridge infrastructure." *Structure and Infrastructure Engineering,* http://dx.doi.org/10.1080/15732479.2010.493304.

[2] Gajer, R.B, Patel, J., and Khazem, D. (1996). "Orthotropic steel deck for the Williamsburg Bridge reconstruction." *Proceedings of the 14th Structures Congress,* 1, 14-18.

[3] American Association of State Highway and Transportation Officials (AASHTO). LRFD Bridge Design Specifications. Washington D.C.

[4] Kozy, B.M., Connor, R.J., Paterson, D., and Mertz, D.R. (2011). "Proposed revisions to AASHTO-LRFD Bridge Design Specifications for Orthotropic Steel Deck Bridges." *Journal of Bridge Engineering,* 16(6), 759-767.

[5] Connor, R., Fisher, J., Gatti, W., Gopalaratnam, V., Kozy, B., Leshko, B., McQuaid, D. L., Medlock, R. Mertz, D., Murphy, T., Paterson, D., Sorensen, O., and Yadlosky, J. (2012). "Manual for design, construction, and maintenance of orthotropic steel deck bridges." *Publication FHWA-IF-12-027.* Washington, D.C.: Federal Highway Administration, US Department of Transportation.

[6] Hobbacher, A. (2005). *Recommendations for fatigue design of welded joints and components. Document XIII-1965-03 / XV-1127-03.* Paris: International Institute of Welding.

[7] Marshall, P.W., and Wardenier, J. (2005). "Tubular versus non-tubular hot spot stress methods." *Proceeding of the 15th International Offshore and Polar Engineering Conference, ISOPE-2005,* June 19-24, Seoul.

[8] Roy, S. and Fisher, J.W. (2005). "Enhancing fatigue strength by Ultrasonic Impact Treatment." *International Journal of Steel Structures,* 5(3), 241–252.

[9] Roy, S., Park, Y.C., Sause, R., Fisher, J.W., and Kaufmann, E.J. (2011). *Cost-effective connection details for highway sign, luminaire and traffic signal structures. NCHRP web-only Document 176.* Washington, D.C.: Transportation Research Board.

[10] Roy, S., Fisher, J.W., Alapati, R.S.D., Manandhar, N.K., and Park, Y.C. (2011). "Fatigue evaluation of orthotropic deck for a signature bridge." *IABSE-IASS Symposium,* September 20–23, London.

[11] Dassault Systèmes. (2011). *Abaqus 6.11: Analysis User's Manual.* Providence, RI: Simulia Corporation.

[12] Roy, S., Alapati, R.S.D., Manandhar, N.K., and Fisher, J.W. (2011). "Measurements of a steel orthotropic deck under crawl loading." *Proceedings of the 2011 ASCE Structures Congress*, April 14–16, Las Vegas.

[13] Connor, R.J., Richards, S.O., and Fisher, J.W. (2003). "Long-term monitoring of prototype orthotropic deck panels on the Bronx-Whitestone Bridge for fatigue evaluation." *Proceedings of the New York City Bridge Conference*, October 20–21, New York City. Lisse:Swets & Zeitlinger.

[14] Connor, R.J., and Fisher, J.W. (2000). "In-service response of an orthotropic steel deck compared with design assumptions" *Transportation Research Record: Journal of the Transportation Research Board,* 1696(13), 100-108..